Published in final edited form as:
Mol Imaging. 2013 ; 12(2): 121–128.

Efficient ^{18}F labeling of cysteine containing peptides and proteins using the tetrazine-*trans*-cyclooctene ligation

Shuanglong Liu[a,‡], **Matthew Hassink**[b,‡], **Ramajeyam Selvaraj**[b], **Li-Peng Yap**[a], **Ryan Park**[a], **Hui Wang**[c], **Xiaoyuan Chen**[c], **Joseph M. Fox**[b], **Zibo Li**[a], and **Peter S. Conti**[a]

Joseph M. Fox: jmfox@udel.edu; Zibo Li: ziboli@usc.edu

[a]Department of Radiology, Keck School of Medicine, Molecular Imaging Center, University of Southern California, Los Angeles, CA 90033, USA. Fax: +1 323 442 3253; Tel: +1 323 442 3253

[b]Brown Laboratories, Department of Chemistry and Biochemistry, University of Delaware, Newark, DE 19803, USA. Fax: +1 302 831 6335; Tel: +1 302 831 0191

[c]Laboratory of Molecular Imaging and Nanomedicine (LOMIN), National Institute of Biomedical Imaging and Bioengineering (NIBIB), National Institutes of Health (NIH), Bethesda, Maryland 20892, USA

Abstract

^{18}F PET has a number of attributes that make it clinically attractive, including nearly 100% positron efficiency, very high specific radioactivity, and short half-life of ~110 min. However, the short half-life of ^{18}F and the poor nucleophilicity of fluoride introduce challenges for the incorporation of ^{18}F into complex molecules. Recently, the tetrazine-*trans*-cyclooctene ligation has been introduced as a novel ^{18}F labeling method that proceeds with fast reaction rates without catalysis. Herein, we report an efficient method for ^{18}F-labeling of free cysteines of peptides and proteins based on sequential ligation with a bifunctional tetrazinyl-maleimide and an ^{18}F-labeled *trans*-cyclooctene. The newly developed method was tested for site specific labeling of both c(RGDyC) peptide and VEGF-SH protein. Starting with 4 mCi of ^{18}F-*trans*-cyclooctene and only 10 μg of tetrazine-RGD (80–100 μM) or 15 μg of tetrazine-VEGF (6.0 μM), ^{18}F labeled RGD peptide and VEGF protein could be obtained within five minutes in 95% yield and 75% yield, respectively. The obtained tracers were then evaluated in mice. In conclusion, a highly efficient method has been developed for site-specific ^{18}F labeling of cysteine containing peptides and proteins. The special characteristics of the tetrazine-*trans*-cyclooctene ligation provide unprecedented opportunities to synthesize ^{18}F-labeled probes with high specific activity for PET applications.

Keywords

^{18}F; tetrazine-*trans*-cyclooctene; PET; Protein labeling; Maleimide

Correspondence to: Joseph M. Fox, jmfox@udel.edu; Zibo Li, ziboli@usc.edu.

‡Equal contributions were made by these authors.

Introduction

High-molecular-weight biological macromolecules, such as single-stranded oligonucleotides [1], peptides [2], and proteins [3], are being considered with increasing frequency for use as radiopharmaceuticals, and the applications of radiolabeled macromolecules are rapidly gaining importance in nuclear medicine. With a half-life of 109.8 min, low β^+-energy (0.64 MeV), and ease of production, ^{18}F-fluoride represents the ideal radionuclides for routine PET imaging. Its low positron energy results in short positron linear range in tissue, which could lead to higher resolution in PET imaging. Furthermore, the half-life of ^{18}F is long enough to allow syntheses, transportation, and imaging procedures to be extended over hours, while the patient is subjected to limited amount of radiation exposure. However, the synthesis of ^{18}F labeled proteins with high specific activity is challenging. ^{18}F-containing prosthetic groups are often required. Moreover, due to the slow rates of conventional conjugation chemistry, a large excess of protein is often required in order to obtain high radiochemical yield. Fast, efficient labeling methods in ^{18}F-radiochemistry are therefore necessary for developing imaging agents in nuclear medicine and life science.

Previously, we and others developed a novel bioconjugation that involves reaction between tetrazines and *trans*-cyclooctenes (TCO) [4–5]. The fast rates of these reactions enable high reactivity at low micromolar concentrations within minutes and without an excess of either reactant [4, 6–7]. With this foundation, we have developed an extremely efficient method for synthesizing ^{18}F-labeled probes with high specific activity based on tetrazines and an ^{18}F-labeled *trans*-cyclooctene (^{18}F-TCO) [8–9]. We also used the tetrazine ligation for the first time in a microPET imaging study using an $\alpha_v\beta_3$ integrin targeted RGD probe that was constructed through this efficient cycloaddition reaction [10]. Recently, this kind of tetrazine/TCO reactions was successfully applied for a pretargeted imaging strategy [6, 11]. These studies demonstrated how the fast rates and efficient reactivity of the tetrazine ligation distinguished it from most existing ^{18}F labeling methods.

In our previous study, the tetrazine functionality was introduced through lysine acylation. A concern for unselective protein modification of lysine residues is possible interference with biologic activity, as the modification of one or more lysines located at or near the active site can reduce the binding affinity. As cysteines are much less abundant than lysine, aspartic acid and glutamic acid residues, thiol-reactive agents can be used to modify peptides and proteins with higher selectivity than amine and carboxylate-reactive reagents. To further explore the scope of the efficient tetrazine ligation, herein we report a new method for ^{18}F-labeling of free cysteine-containing bioligands. The newly developed method was tested for site specific labeling of c(RGDyC) and VEGF-SH protein.

Materials and Methods

General

All chemicals obtained commercially were of analytic grade and used without further purification. No-carrier-added ^{18}F-fluoride was produced via the ^{18}O(p,n)^{18}F reaction by the bombardment of an isotopically enriched [^{18}O]water target (95% enrichment, Isonics, Golden, CO) with 11-MeV protons using a Siemens RDS-112 negative ion cyclotron.

Reversed-phase extraction C18 Sep-Pak cartridges were obtained from Waters (Milford MA) and were pretreated with ethanol and water immediately before use. The syringe filter and polyethersulfone membranes (pore size, 0.22 μm; diameter, 13 mm) were obtained from Nalge Nunc International (Rochester, NY). c(RGDyC) was obtained from Peptides International (Louisville, KY). The protein VEGF-SH was provided by Dr. Xiaoyuan Chen at NIH. The semipreparative reversed-phase high performance liquid chromatography (RP-HPLC) using a Vydac protein and peptide column (218TP510; 5 μm, 250 × 4.6 mm) was performed on a Dionex 680 chromatography system with a UVD 170U absorbance detector and model 105S single-channel radiation detector (Carroll & Ramsey Associates). The recorded data were processed using Chromeleon version 7.1 software. With a flow rate of 1.0 mL/min, the mobile phase was changed from 95% solvent A [0.1% trifluoroacetic acid (TFA) in water] and 5% B [0.1% TFA in acetonitrile (MeCN)] (0–2 min) to 5% solvent A and 95% solvent B at 22 min. UV absorbance was monitored at 218 nm and the identification of the peptides were confirmed based on the UV spectrum using a photodiode array detector. MicroPET scans were performed on a microPET R4 rodent model scanner (Siemens Medical Solutions USA, Inc., Knoxville, TN). The scanner has a computer-controlled bed and 10.8-cm transaxial and 8-cm axial fields of view (FOVs). It has no septa and operates exclusively in the 3-dimensional (3D) list mode. Animals were placed near the center of the FOV of the scanner.

Chemistry

Synthesis of *N*1-(2-(2,5-dioxo-2,5-dihydro-1H-pyrrol-1-yl)ethyl)-*N*5-(6-(6-(pyridin-2-yl)-1,2,4,5-tetrazin-3-yl)pyridin-3-yl)glutaramide [Tetrazinyl Maleimide (TM)]

A flame dried flask was charged with 2,5-dioxopyrrolidin-1-yl 5-oxo-5-((6-(6-(pyridin-2-yl)-1,2,4,5-tetrazin-3-yl)pyridin-3-yl)amino)pentanoate (*7*) 0.030 g (0.065 mmol) and N-(2-aminoethyl)maleimide trifluoroacetate salt 0.020 g (0.078 mmol). The flask was evacuated and then refilled with nitrogen. Anhydrous *N*,*N*-Dimethylformamide (1 mL) was added and the mixture was stirred. Diisopropylethylamine (0.032 mL, 0.195 mmol) was added dropwise to the mixture. The reaction was stirred for 24 h. at room temperature. The reaction was condensed in vacuo then loaded onto a silica gel column and then run using a gradient of 0–10% MeOH in CH_2Cl_2 as the eluent to give 0.015g (0.031 mmol, 48%) of the title compound as dark red solid. ^{1}H NMR (400 MHz, DMSO-d6) δ 10.56 (s, 1H), 9.06 (s, 1H), 8.94 (d, *J* = 4.3 Hz, 1H), 8.65-8.58 (m, 2H), 8.45-8.41 (m, 1H), 8.16 (t, *J* = 7.8 Hz, 1H), 7.99-7.93 (m, 1H), 7.76-7.70 (m, 1H), 7.01 (s, 2H) 3.49-3.43 (m, 2H), 3.24-3.17 (m, 2H), 2.42 (t, *J* = 7.22 Hz, 2H), 2.09 (t, *J* = 7.5 Hz, 2H), 1.86-1.78 (m, 2H); ^{13}C NMR (100 MHz, DMSO) δ 172.7 (C), 172.5 (C), 171.6 (C), 163.5 (C), 163.2 (C), 151.1 (CH), 150.7 (C), 144.2 (C), 141.7 (C), 139.0 (C) 138.3 (CH), 135.0 (CH), 127.1 (CH), 126.6 (CH), 125.4 (CH), 124.7 (CH), 37.7 (CH_2), 37.3 (CH_2), 36.1 (CH_2), 34.9 (CH_2), 21.1 (CH_2); HRMS-ESI *m/z*: [M+H] calcd for $C_{23}H_{22}N_9O_4$, 488.1795; found 488.1796.

Synthesis of ^{19}F-TTM-RGD

The conjugation was modeled after a reported procedure [12]. Thus, the tetrazinyl-maleimide (TM, 200 μg, 0.41 μmol) in 100 μL dimethyl sulfoxide (DMSO) and c(RGDyC) (200 μg, 0.33 μmol) in 500 μL phosphate buffer (50 mM, pH 6.5–7.0) were mixed together

at room temperature. After the mixture was stirred for 5 h, the tetrazinyl-maleimide-RGD conjugate (TM-RGD) was purified by semipreparative HPLC. The collected fractions were combined and lyophilized to afford a pink powder. TM-RGD was obtained in 85% yield.

^{19}F-TCO was synthesized according to our previous report [8]. TM-RGD (100 μg, 92 nmol, in 100 μL DMSO) and ^{19}F-TCO (200 μg, 0.33 μmol, in 100 μL DMSO) were mixed together at room temperature. After the mixture was stirred for 5 min, the conjugate was purified by semipreparative HPLC. The collected fractions were combined and lyophilized to afford the final product as a white powder. ^{19}F-TTM-RGD was obtained in 92% yield with 13.2 min retention time on analytical HPLC. MALDI-TOF-MS (*m/z*): $[M + H]^+$ calcd for $C_{57}H_{73}FN_{15}O_{13}S$, 1226.5; found 1226.4.

Synthesis of ^{18}F-TTM-RGD via Cycloaddition of ^{18}F-TCO and TM-RGD

^{18}F-TCO (148 MBq, 4 mCi, in 50 μL ethanol) was added to the TM-RGD solution (10 μg, in 50 μL DMSO) followed by 5 min incubation at 40 °C. The conjugate of ^{18}F-TCO and TM-RGD, referred to as ^{18}F-TTM-RGD, was purified by semipreparative HPLC. The collected fractions were combined and the solvent was removed by rotary evaporation under reduced pressure. ^{18}F-TTM-RGD was reconstituted in 1 mL phosphate buffered saline (PBS) and passed through a 0.22 μm syringe filter for *in vivo* animal experiments.

Synthesis of ^{18}F-TTM-VEGF

The tetrazinyl-maleimide (TM, 200 μg, 0.41 μmol, in 100 μL DMSO) and VEGF-SH (100 μg, 5.5 nmol, in 500 μL phosphate buffer) were mixed together at room temperature for 5 h. The conjugate was purified by size exclusion PD-10 column and concentrated by Centricon filter (Millipore, Bedford, MA). The final concentration of tetrazinyl-maleimide-VEGF conjugate (TM-VEGF) was determined based on UV absorbance at 280 nm using unconjugated VEGF of known concentrations as standards. The final concentration was then adjusted to 50 μg/mL. For ^{18}F labeling, ^{18}F-TCO (148 MBq, 4 mCi, in 50 μL ethanol) was added to the TM-VEGF (15 μg) in water and incubated for 5 min at 40 °C. The conjugate (shortened as ^{18}F-TTM-VEGF) was purified by PD-10 column using 1×PBS as the eluent. The 3.0–4.0 mL fraction containing VEGF proteins were collected for *in vivo* animal experiments.

Cell Culture

Human glioblastoma cell line U87MG was obtained from the American Type Culture Collection (Manassas, VA) and were cultured in DMEM containing high glucose (GIBCO, Carlsbad, CA), which was supplemented with 10% fetal bovine serum (FBS) and 1% penicillin-streptomycin. The cells were expanded in tissue culture dishes and kept in a humidified atmosphere of 5% CO_2 at 37 °C. The medium was changed every other day. A confluent monolayer was detached with 0.05% Trypsin-EDTA, 0.01M PBS (pH 7.4) and dissociated into a single-cell suspension for further cell culture.

MicroPET Imaging

Animal procedures were performed according to a protocol approved by the University of Southern California Institutional Animal Care and Use Committee. For static microPET

scans, the mice bearing U87MG xenografts were injected with 3.7 MBq (100 μCi) of ^{18}F-TTM-RGD *via* the tail vein (n = 3 for each group). At 0.5, 1, and 2 h post injection (p.i.), the mice were anesthetized with isoflurane (5% for induction and 2% for maintenance in 100% O_2) using a knock-down box. With the help of a laser beam attached to the scanner, the mice were placed in the prone position and near the center of the field of view of the scanner. The 3-min static scans were then obtained. Images were reconstructed using a 2-dimensional ordered-subsets expectation maximization (OSEM) algorithm. Regions of interest (ROIs; 5 pixels for coronal and transaxial slices) were drawn over the tumor on decay-corrected whole-body coronal images. The maximum counts per pixel per minute were obtained from the ROI and converted to counts per milliliter per minute using a calibration constant. With the assumption of a tissue density of 1 g/mL, the ROIs were converted to counts per gram per min. Image ROI-derived %ID/g values were determined by dividing counts per gram per minute with injected dose. Similarly, 3.7 MBq (100 μCi) of ^{18}F-TTM-VEGF was injected to healthy nude mice to study its distribution with microPET. Static scans were performed at 0.5 h and 3 h post injection.

Results

Chemistry and Radiochemistry

The synthesis of the bifunctional tetrazinyl-maleimide (TM) is shown in Figure 1, and the syntheses of RGD conjugates are shown in Figure 2A. The conjugation of the bifunctional tetrazinyl-maleimide (TM) with c(RGDyC) in phosphate buffer with pH 6.5–7.0 afforded the tetrazinyl-maleimide-RGD conjugate TM-RGD in 85% yield. The cycloaddition reaction of TM-RGD and nonradioactive ^{19}F-TCO provided the standard for the ^{18}F labeled product. The pink color of TM-RGD disappeared immediately upon the addition of ^{19}F-TCO, indicating that the tetrazine had completely reacted upon mixing. The identity of the ^{19}F-TTM-RGD was confirmed by MALDI-TOF-MS. ^{18}F labeled *trans*-cyclooctene (^{18}F-TCO) was produced using the protocol developed in our laboratories [8]. The radiolabeling yield for ^{18}F-TTM-RGD was counted nearly quantitatively from ^{18}F-TCO (Figure 3A). The radiochemical purity of ^{18}F-TTM-RGD was more than 95% as determined by radio HPLC. The specific activity of ^{18}F-TTM-RGD was estimated to be approximately 3–6 Ci/μmol. Following a similar protocol, ^{18}F-TTM-VEGF was obtained in high yield (75% after purification) from VEGF-SH.

To compare the efficiency of the tetrazine ligation with direct conjugate addition of a sulfhydryl containing peptide to a maleimide, we performed the reaction between ^{18}F-TCO and the tetrazinyl maleimide TM directly, which produced the cycloadduct ^{18}F-TTM (Fig 1B). The conjugate ^{18}F-TTM-RGD could also be efficiently obtained through the reaction of ^{18}F-TTM and c(RGDyC); however, a relatively long reaction time (20 min) and a higher concentration of c(RGDyC) (1.8 mM) was needed. By contrast, the approach outlined in Fig 1A requires fewer manipulations of ^{18}F-labeled intermediates, and is complete within 5 min at room temperature at a concentration that is 18 times lower (0.1 mM).

MicroPET Imaging

Representative coronal microPET images of U87MG tumor-bearing mice (n = 3/group) at different times after intravenous injection of approximately 3.7 MBq (100 μCi) of ^{18}F-TTM-RGD are shown in Figure 4A. The tumors were clearly visible with good contrast at all time points. The mice showed high abdominal activity accumulation. Prominent uptake of ^{18}F-TTM-RGD was observed in the kidneys and urinary bladder at early time points, indicating that this radiotracer is excreted through the renal system as well. Quantification of tumor and major organ activity accumulation in the microPET scans was achieved by measuring the regions of interest (ROIs) that encompass the entire organ on the coronal images. The tumor and major organ uptake of ^{18}F-TTM-RGD is depicted in Figure 5A. The tumor uptake of ^{18}F-TTM-RGD in U87MG tumor was 1.98 ± 0.33, 1.80 ± 0.15, and 1.27 ± 0.33 %ID/g at 0.5, 1, and 2 h p.i., respectively. As can be seen from Figure 5A, the uptake of the ^{18}F-TTM-RGD decreased rapidly with time in the muscle, which afforded a better contrast at late time points (2 h p.i.).

The biodistribution of ^{18}F-TTM-VEGF was evaluated in normal Sprague Dawley nude mice. Representative coronal microPET images and the 2D projections at 0.5 and 3 h post injection of about 3.7 MBq (100 μCi) ^{18}F-TTM-VEGF are shown in Figure 4B, 4C. The activity was mainly accumulated in kidneys, which correlated well with a previous report [13]. MicroPET quantification was performed by measuring the ROI and the result is shown in Figure 5B. The kidney uptake of ^{18}F-TTM-VEGF was 23.20 ±2.15 and 16.51 ± 1.52 %ID/g at 0.5 h and 3 h post injection, respectively. Low muscle uptakes were observed (2.98 ± 0.66 and 1.59 ± 0.57 %ID/g at 0.5 and 3 h post injection).

Discussion

The development of ^{18}F labeled PET probes is rapidly gaining importance in nuclear medicine. ^{18}F-fluoride is generally incorporated into the bioligands through three types of functional groups: amino groups [14–16], carboxylic acid groups [17], and sulfhydryl groups. As cysteines are much less abundant than lysines, aspartic acid, and glutamic acid residues, thiol-reactive agents have been used to site-selectively modify peptides and proteins [18–19]. Previously, several thiol-reactive ^{18}F-synthons have been reported, all of which bear a maleimide group for conjugate addition of thiols under mild conditions [12, 20–22]. These labeling methods use mild reaction conditions and give high radiolabeling yields. However, the preparation of ^{18}F-fluorinated probes by conventional methods requires a relatively large amount of bioligand (100–1000 μg) in the bioconjugation step. For peptides or proteins with high cost and low availability, it is desirable to minimize the amount of wasted ligand. Furthermore, for large peptides and for protein labeling, the unlabeled ligands cannot necessarily be efficiently separated from the ^{18}F-labeled ligands. As unlabeled ligands are competitive inhibitors of the ^{18}F-labeled probes, the unlabeled ligands can dramatically decrease the sensitivity of radiolabeling. Thus, it is a premium consideration to decrease the equivalency of labeling precursor while maintaining fast and efficient reactivity.

In this study, we developed a bifunctional tetrazinyl-maleimide (TM) that is capable of selectively introducing tetrazine functionality to bioligands through the sulfhydryl group,

and subsequent bioconjugation with ^{18}F-TCO. In order to evaluate the new labeling method, two ligands, c(RGDyC) and VEGF-SH, were selected for labeling reaction.

The conjugation between TM and c(RGDyC) or VEGF-SH is efficient at room temperature. After purification, the radiolabeling of TM-RGD and TM-VEGF was performed with low loadings of bio-ligands. Starting from ^{18}F-TCO, the synthesis of ^{18}F-TTM-RGD was achieved in nearly quantitative yield. The total radiosynthesis time was about 90 min from the end of bombardment. For ^{18}F-TTM-VEGF, the 75% labeling yield was calculated by collecting and measuring the radioactivity from intermediate fractions (3–4 mL) that eluted from a PD-10 size-exclusion column (Later fractions were excluded from the yield calculation).

Previously, several thiol reactive ^{18}F-tagging molecules have been described [12, 20–22], all of which bear a maleimide group allowing for thiol-specific Michael addition reaction. The total synthesis time of those ^{18}F-tags range from 100–150 min with 10%–20% non-decay corrected radiochemical yields. As ^{18}F-TCO can be prepared with a total synthesis time of 50 min and in 71% radiochemical yield, the present method represents an efficient alternative for the introduction of ^{18}F-labels to the sulfhydryl functions of biological molecules.

In the microPET study, ^{18}F-TTM-RGD was found to accumulate in U87MG tumor, which is consistent with our previous PET RGD studies [23–25]. The tumor uptake of ^{18}F-TTM-RGD in U87MG tumor was 1.98 ± 0.33, 1.80 ± 0.15, and 1.27 ± 0.33 % ID/g at 0.5, 1, and 2 h p.i., respectively. Compared with the *N*-succinimidyl-4-[^{18}F]fluorobenzoate (^{18}F-SFB) labeled RGD (^{18}F-FB-RGD) [25], the tumor uptakes were slightly higher. However, the uptakes of normal organs such as kidneys and liver are also higher than those of 4-[^{18}F]fluorobenzoate- labeled RGD (^{18}F-FB-RGD). For example, the liver uptake was 0.39 ± 0.05 %ID/g for ^{18}F-FB-RGD and 2.35 ± 0.24 %ID/g for ^{18}F-TTM-RGD at 2 h p.i. The higher uptake in liver might be attributed to the increased lipophilicity of ^{18}F-TTM-RGD as hydrophilic polyethylene glycol (PEG) linkers in order to decrease the liver uptake.

In addition to RGD peptides, we also tested our method for protein labeling. The interaction between VEGF and its receptor (VEGFR) has been extensively studied for angiogenesis-related pathways, which are very important for the tumor growth [26–29]. Previously, VEGF protein based tracers have been developed for PET, single photon emission computed tomography (SPECT) and optical imaging of tumor angiogenesis, all of which showed high renal uptake due to the VEGF-R1 receptor expression in kidneys [30–34]. In the present study, we evaluated the ^{18}F-TTM-VEGF in normal mice and the biodistribution pattern correlates well with previous reports. The kidney uptake was 23.20 ± 2.15 and 16.51 ± 1.52 %ID/g at 0.5 and 3 h p.i., respectively (Figure 5B). The high kidney uptake is consistent with the literature [13, 27, 35–36]. These results indicate that the radiolabeling was successful and the labeling moiety had a minimum effect on VEGF binding to its receptor. In conclusion, a highly efficient method has been developed for site-specific ^{18}F labeling of cysteine containing peptides and proteins. The special characteristics of the tetrazine-*trans*-cyclooctene ligation provide unprecedented opportunities to synthesize ^{18}F-labeled probes with high specific activity for PET applications.

Conclusions

Despite the great potential of using ^{18}F-labeled proteins for both diagnoses and therapeutic monitoring, their application has been limited because it is very challenging to synthesize ^{18}F-labeled proteins in adequate yield with high specific activity. In this study, we developed an efficient method for the construction of ^{18}F labeled proteins with high specific activity based on the tetrazine-*trans*-cyclooctene ligation. We demonstrated that tetrazinyl-maleimide can conjugate with peptides and proteins bearing a free cysteine residue and that the resulting bioconjugates can be efficiently ^{18}F-labeled through ^{18}F-TCO ligation. The major advantage of this strategy lies in the fact that this cycloaddition reaction is highly efficient and enables very low bioligand loading. This tetrazinyl maleimide reagent should be useful for the labeling of a variety of peptides, proteins, or oligonucleotides containing free sulfhydryl groups. Future studies will be directed toward the creation of even more reactive bioconjugation partners, and improving the selectivity for tumor uptake relative to kidney uptake. This advance in ^{18}F labeling methodology should enable the discovery of critical imaging probes for cancer diagnosis and treatment monitoring in both basic and clinical research.

Acknowledgments

This work was supported by NIH Grant Number P20 RR017716 from the COBRE Program of the NCRR, P30CA014089 from the National Cancer Institute, research grant DE-SC0002353 from the Department of Energy, and by the USC Department of Radiology. Spectra were obtained with instrumentation supported by NSF CRIF:MU grants: CHE 0840401 and CHE-0541775.

References

1. Dewanjee MK, Haider N, Narula J. Imaging with radiolabeled antisense oligonucleotides for the detection of intracellular messenger RNA and cardiovascular disease. J Nucl Cardiol. 1999; 6:345–56. [PubMed: 10385190]
2. Maecke HR. Radiolabeled peptides in nuclear oncology: influence of peptide structure and labeling strategy on pharmacology. Ernst Schering Res Found Workshop. 2005:43–72. [PubMed: 15524210]
3. Kilbourn MR, Dence CS, Welch MJ, et al. Fluorine-18 labeling of proteins. J Nucl Med. 1987; 28:462–70. [PubMed: 3494825]
4. Blackman ML, Royzen M, Fox JM. Tetrazine ligation: fast bioconjugation based on inverse-electron-demand Diels-Alder reactivity. J Am Chem Soc. 2008; 130:13518–9. [PubMed: 18798613]
5. Devaraj NK, Weissleder R. Biomedical applications of tetrazine cycloadditions. Acc Chem Res. 2011; 44:816–27. [PubMed: 21627112]
6. Rossin R, Verkerk PR, van den Bosch SM, et al. In vivo chemistry for pretargeted tumor imaging in live mice. Angew Chem Int Ed Engl. 2010; 49:3375–8. [PubMed: 20391522]
7. Devaraj NK, Upadhyay R, Haun JB, et al. Fast and sensitive pretargeted labeling of cancer cells through a tetrazine/trans-cyclooctene cycloaddition. Angew Chem Int Ed Engl. 2009; 48:7013–6. [PubMed: 19697389]
8. Li Z, Cai H, Hassink M, et al. Tetrazine-trans-cyclooctene ligation for the rapid construction of ^{18}F labeled probes. Chem Commun (Camb). 2010; 46:8043–5. [PubMed: 20862423]
9. Keliher EJ, Reiner T, Turetsky A, et al. High-yielding, two-step ^{18}F labeling strategy for ^{18}F-PARP1 inhibitors. ChemMedChem. 2011; 6:424–7. [PubMed: 21360818]
10. Selvaraj R, Liu S, Hassink M, et al. Tetrazine-trans-cyclooctene ligation for the rapid construction of integrin $\alpha_v\beta_3$ targeted PET tracer based on a cyclic RGD peptide. Bioorg Med Chem Lett. 2011; 21:5011–4. [PubMed: 21601452]

11. Devaraj NK, Thurber GM, Keliher EJ, et al. Reactive polymer enables efficient in vivo bioorthogonal chemistry. Proc Natl Acad Sci U S A. 2012; 109:4762–7. [PubMed: 22411831]
12. Cai W, Zhang X, Wu Y, et al. A thiol-reactive ^{18}F-labeling agent, N-[2-(4-^{18}F-fluorobenzamido)ethyl]maleimide, and synthesis of RGD peptide-based tracer for PET imaging of $\alpha_v\beta_3$ integrin expression. J Nucl Med. 2006; 47:1172–80. [PubMed: 16818952]
13. Willmann JK, Chen K, Wang H, et al. Monitoring of the biological response to murine hindlimb ischemia with ^{64}Cu-labeled vascular endothelial growth factor-121 positron emission tomography. Circulation. 2008; 117:915–22. [PubMed: 18250264]
14. Mittra ES, Goris ML, Iagaru AH, et al. Pilot Pharmacokinetic and Dosimetric Studies of ^{18}F-FPPRGD$_2$: A PET Radiopharmaceutical Agent for Imaging $\alpha_v\beta_3$ Integrin Levels. Radiology. 2011; 260:182–91. [PubMed: 21502381]
15. Haubner R, Weber WA, Beer AJ, et al. Noninvasive visualization of the activated $\alpha_v\beta_3$ integrin in cancer patients by positron emission tomography and [^{18}F]Galacto-RGD. PLoS Med. 2005; 2:e70. [PubMed: 15783258]
16. Beer AJ, Haubner R, Goebel M, et al. Biodistribution and pharmacokinetics of the $\alpha_v\beta_3$-selective tracer ^{18}F-galacto-RGD in cancer patients. J Nucl Med. 2005; 46:1333–41. [PubMed: 16085591]
17. Shai Y, Kirk KL, Channing MA, et al. ^{18}F-labeled insulin: a prosthetic group methodology for incorporation of a positron emitter into peptides and proteins. Biochemistry. 1989; 28:4801–6. [PubMed: 2669963]
18. Brinkley M. A brief survey of methods for preparing protein conjugates with dyes, haptens, and cross-linking reagents. Bioconjug Chem. 1992; 3:2–13. [PubMed: 1616945]
19. Wilbur DS. Radiohalogenation of proteins: an overview of radionuclides, labeling methods, and reagents for conjugate labeling. Bioconjug Chem. 1992; 3:433–70. [PubMed: 1463775]
20. de Bruin B, Kuhnast B, Hinnen F, et al. 1-[3-(2-[^{18}F]fluoropyridin-3-yloxy)propyl]pyrrole-2,5-dione: design, synthesis, and radiosynthesis of a new [^{18}F]fluoropyridine-based maleimide reagent for the labeling of peptides and proteins. Bioconjug Chem. 2005; 16:406–20. [PubMed: 15769096]
21. Shiue CY, Wolf AP, Hainfeld JF. Synthesis of ^{18}F-labelled N-(p-[^{18}F]fluorophenyl) maleimide and its derivatives for labelling monoclonal antibody with ^{18}F. J Labelled Compds Radiopharm. 1998; 26:287–9.
22. Toyokuni T, Walsh JC, Dominguez A, et al. Synthesis of a new heterobifunctional linker, N-[4-(aminooxy)butyl]maleimide, for facile access to a thiol-reactive ^{18}F-labeling agent. Bioconjug Chem. 2003; 14:1253–9. [PubMed: 14624642]
23. Chen X, Park R, Khankaldyyan V, et al. Longitudinal microPET imaging of brain tumor growth with F-18-labeled RGD peptide. Mol Imaging Biol. 2006; 8:9–15. [PubMed: 16315003]
24. Chen X, Park R, Shahinian AH, et al. ^{18}F-labeled RGD peptide: initial evaluation for imaging brain tumor angiogenesis. Nucl Med Biol. 2004; 31:179–89. [PubMed: 15013483]
25. Chen X, Park R, Tohme M, et al. MicroPET and autoradiographic imaging of breast cancer α_v-integrin expression using ^{18}F- and ^{64}Cu-labeled RGD peptide. Bioconjug Chem. 2004; 15:41–9. [PubMed: 14733582]
26. Folkman J. Angiogenesis in cancer, vascular, rheumatoid and other disease. Nat Med. 1995; 1:27–31. [PubMed: 7584949]
27. Cai W, Chen X. Multimodality imaging of vascular endothelial growth factor and vascular endothelial growth factor receptor expression. Front Biosci. 2007; 12:4267–79. [PubMed: 17485373]
28. Ferrara N. VEGF and the quest for tumour angiogenesis factors. Nat Rev Cancer. 2002; 2:795–803. [PubMed: 12360282]
29. Ferrara N. Vascular endothelial growth factor: basic science and clinical progress. Endocr Rev. 2004; 25:581–611. [PubMed: 15294883]
30. Wang H, Cai W, Chen K, et al. A new PET tracer specific for vascular endothelial growth factor receptor 2. Eur J Nucl Med Mol Imaging. 2007; 34:2001–10. [PubMed: 17694307]
31. Backer MV, Levashova Z, Patel V, et al. Molecular imaging of VEGF receptors in angiogenic vasculature with single-chain VEGF-based probes. Nat Med. 2007; 13:504–9. [PubMed: 17351626]

32. Blankenberg FG, Mandl S, Cao YA, et al. Tumor imaging using a standardized radiolabeled adapter protein docked to vascular endothelial growth factor. J Nucl Med. 2004; 45:1373–80. [PubMed: 15299064]

33. Blankenberg FG, Backer MV, Levashova Z, et al. In vivo tumor angiogenesis imaging with site-specific labeled ^{99m}Tc-HYNIC-VEGF. Eur J Nucl Med Mol Imaging. 2006; 33:841–8. [PubMed: 16699765]

34. Chan C, Sandhu J, Guha A, et al. A human transferrin-vascular endothelial growth factor (hnTf-VEGF) fusion protein containing an integrated binding site for ^{111}In for imaging tumor angiogenesis. J Nucl Med. 2005; 46:1745–52. [PubMed: 16204726]

35. Cai W, Chen K, Mohamedali KA, et al. PET of vascular endothelial growth factor receptor expression. J Nucl Med. 2006; 47:2048–56. [PubMed: 17138749]

36. Chen K, Cai W, Li ZB, et al. Quantitative PET imaging of VEGF receptor expression. Mol Imaging Biol. 2009; 11:15–22. [PubMed: 18784964]

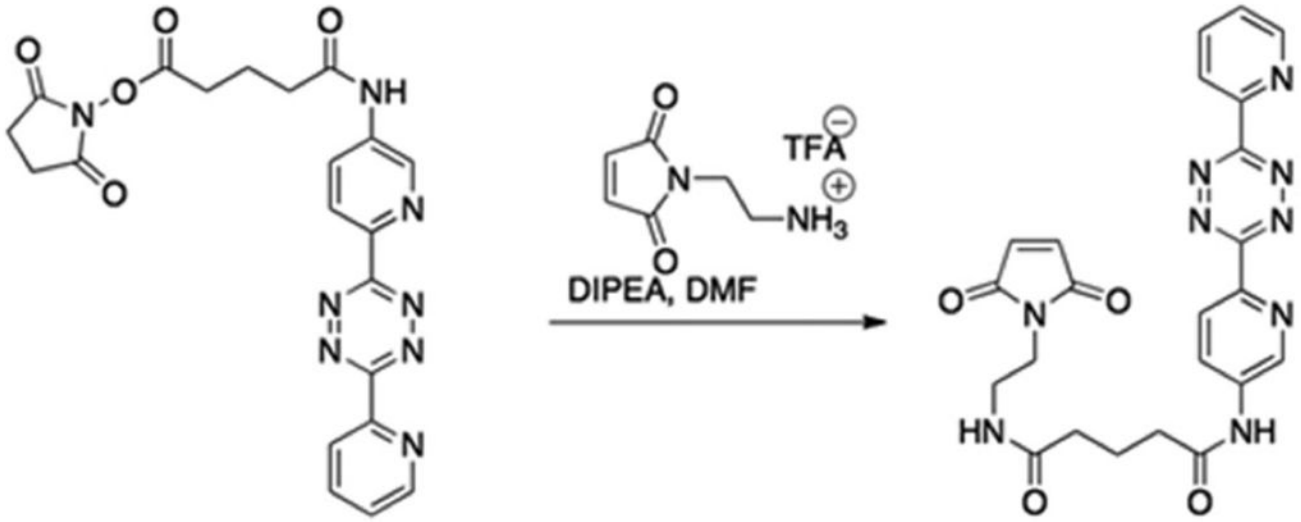

Figure 1.
Synthesis of N1-(2-(2,5-dioxo-2,5-dihydro-1H-pyrrol-1-yl)ethyl)-N5-(6-(6-(pyridin-2-yl)-1,2,4,5-tetrazin-3-yl)pyridin-3-yl)glutaramide

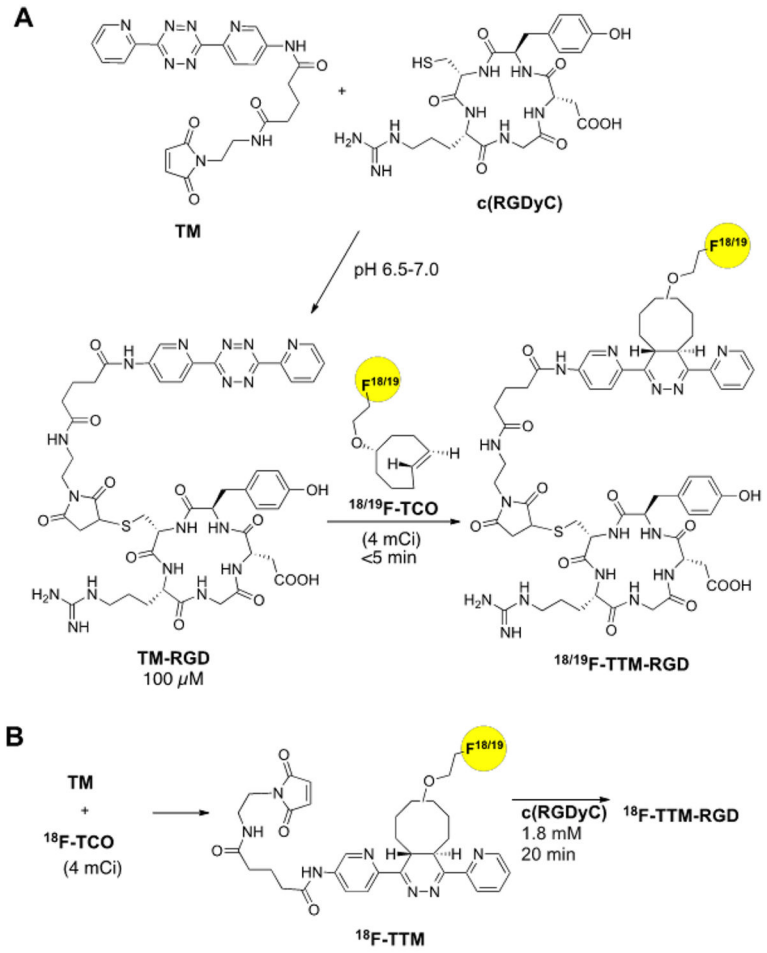

Figure 2.

The different synthesis routes for $^{18/19}$F-TTM-RGD. (A) Synthesis of TM-RGD followed by ^{18}F labeling with ^{18}F-TCO. (B) Synthesis of ^{18}F-TTM followed by c(RGDyC) conjugation.

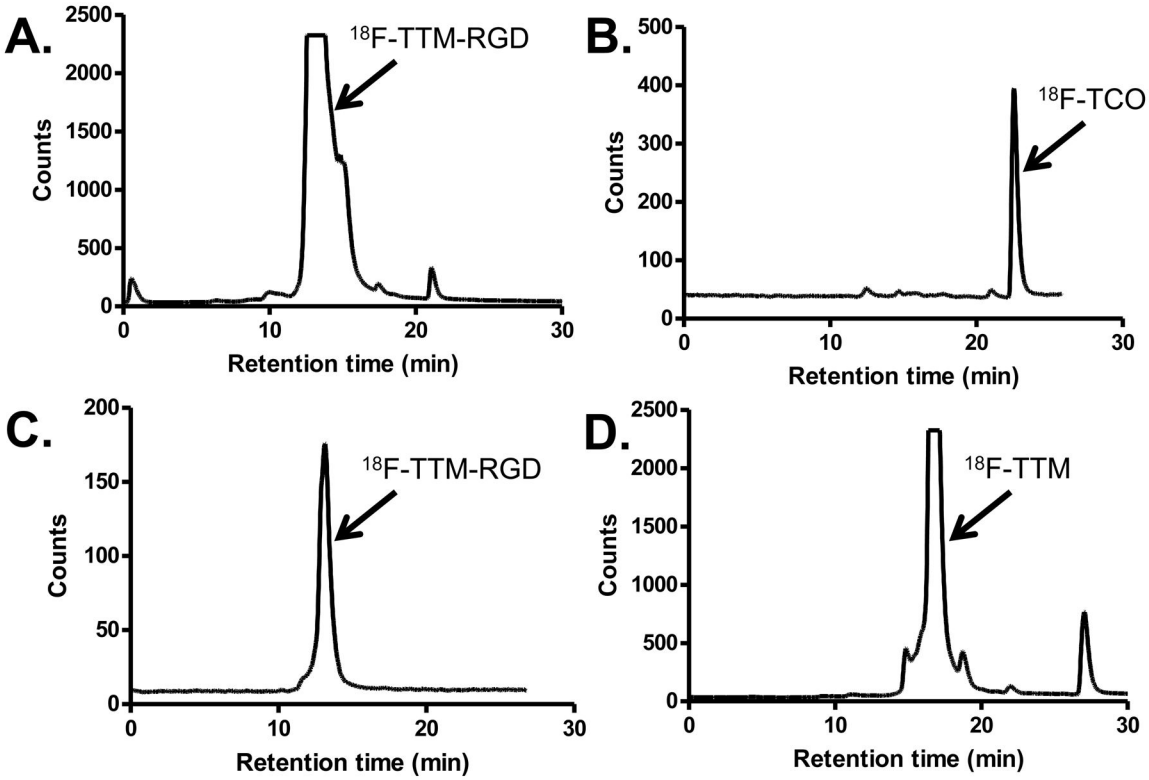

Figure 3.

The radioHPLC profiles of ^{18}F-TTM-RGD purification and quality control (QC). (A) Purification of the crude mixture of ^{18}F-TCO and TM-RGD. (B) The QC of ^{18}F-TCO. (C) The QC of ^{18}F-TTM-RGD. (D) The purification radioHPLC profile for the crude mixture of ^{18}F-TCO and tetrazine-maleimide.

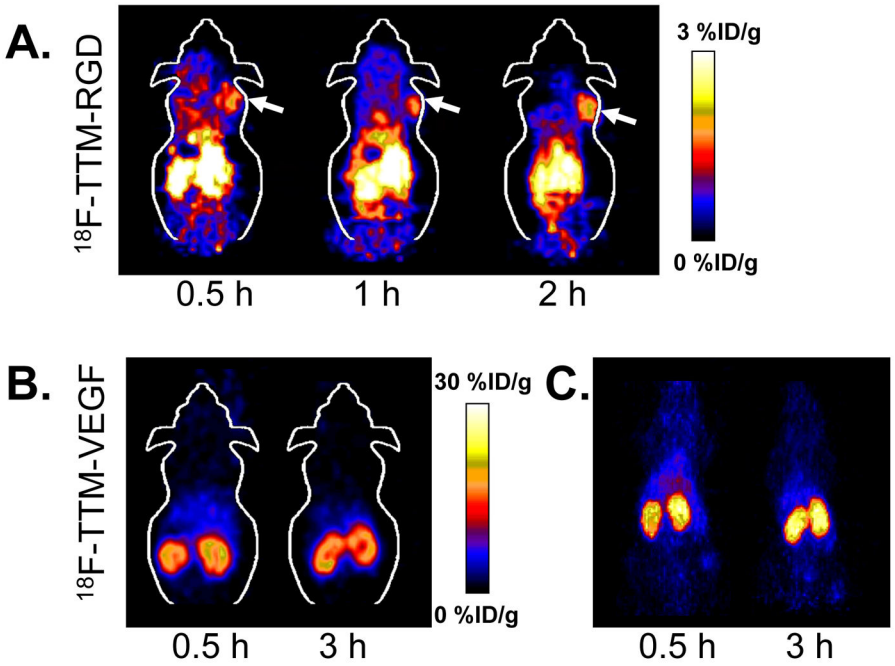

Figure 4.

(A) Decay-corrected whole-body coronal microPET images of athymic female nude mice bearing U87MG tumor from a static scan at 0.5 h, 1 h, and 2 h after injection of ^{18}F-TTM-RGD. Tumors are indicated by arrows. (B) Decay-corrected whole-body coronal microPET images of normal athymic female nude mice from a static scan at 0.5 h, and 3 h after injection of ^{18}F-TTM-VEGF. (C) 2D projection of the microPET images of athymic female nude mice after injection of ^{18}F-TTM-VEGF.

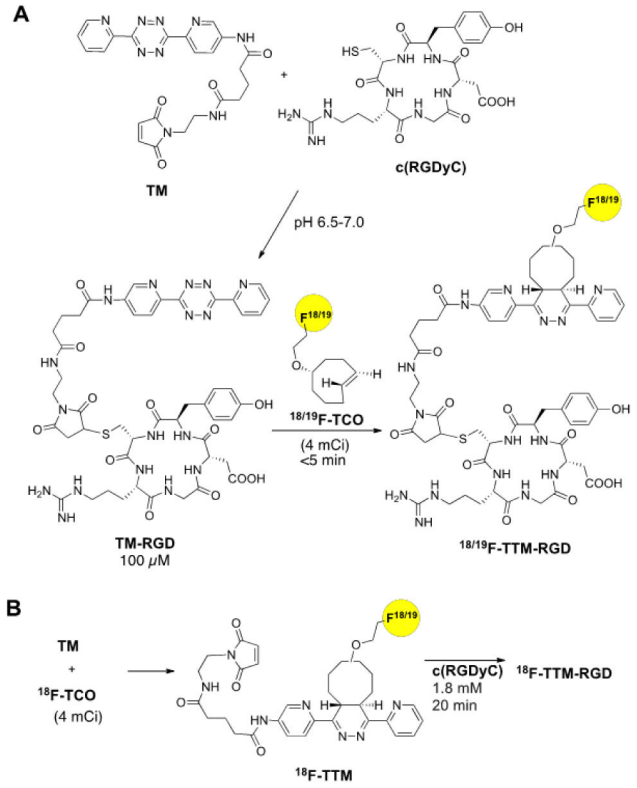

Figure 5.

MicroPET quantification of tumor and major organs after injection of (A) ^{18}F-TTM-RGD and (B) ^{18}F-TTM-VEGF, respectively.